AIP | Journal of Applied Physics

On the effect of the barrier widths in the InAs/AlSb/GaSb singlebarrier interband tunneling structures

J. F. Chen, L. Yang, M. C. Wu, S. N. G. Chu, and A. Y. Cho

Citation: Journal of Applied Physics **68**, 3451 (1990); doi: 10.1063/1.346355
View online: http://dx.doi.org/10.1063/1.346355
View Table of Contents: http://scitation.aip.org/content/aip/journal/jap/68/7?ver=pdfcov
Published by the AIP Publishing

Articles you may be interested in

Proton irradiation of InAs/AlSb/GaSb resonant interband tunneling diodes
Appl. Phys. Lett. **78**, 2581 (2001); 10.1063/1.1363697

Carrier transport in InAs/AlSb/GaSb interband tunneling structures
J. Appl. Phys. **74**, 6222 (1993); 10.1063/1.355195

Quantization effect on capacitancevoltage and currentvoltage characteristics of an InAs/AlSb/GaSb interband tunneling diode
J. Appl. Phys. **68**, 4286 (1990); 10.1063/1.346222

InAs/AlSb/GaSb singlebarrier interband tunneling diodes with high peaktovalley ratios at room temperature
J. Appl. Phys. **68**, 3040 (1990); 10.1063/1.346396

Interband tunneling in singlebarrier InAs/AlSb/GaSb heterostructures
Appl. Phys. Lett. **56**, 952 (1990); 10.1063/1.102634

AIP | Journal of Applied Physics

Journal of Applied Physics is pleased to announce André Anders as its new Editor-in-Chief

[This article is copyrighted as indicated in the article. Reuse of AIP content is subject to the terms at: http://scitation.aip.org/termsconditions. Downloaded to] IP: 128.32.46.241 On: Mon, 21 Jul 2014 20:13:05

On the effect of the barrier widths in the InAs/AlSb/GaSb single-barrier interband tunneling structures

J. F. Chen, L. Yang, M. C. Wu, S. N. G. Chu, and A. Y. Cho
AT&T Bell Laboratories, Murray Hill, New Jersey 07974

(Received 26 February 1990; accepted for publication 7 June 1990)

The dependence of the interband tunneling current on AlSb barrier widths is studied in the InAs/AlSb/GaSb single-barrier diode structures. The experimental results show that the peak current density displays an exponential dependence on the barrier width. The Wentzel-Kramers-Brillouin approximation combined with the $k \cdot p$ two-band model were used in analyzing the energy level in the AlSb barrier through which the peak tunneling currents occur. The energy level thus obtained (0.48 ± 0.10 eV above the valence band edge of the AlSb) agrees with the valence-band offset (0.40 ± 0.15 eV) between the AlSb and the GaSb obtained by x-ray photoemission measurement reported by Gualtieri *et al.* [Appl. Phys. Lett. **49**, 1037 (1986)]. By adjusting the barrier width properly, we obtained a high peak current density of 24 kA/cm^2 (with a peak-to-valley ratio of 1.4) and a high peak-to-valley ratio of 4.5 (with a peak current density of 3.5 kA/cm^2) at room temperature. In addition, the peak-current voltages for different AlSb barrier widths were calculated and compared with the measured results.

I. INTRODUCTION

Among III-V compound semiconductors, the InAs/AlSb/GaSb represents a material system closely matching in lattice constant, yet significantly differing in band parameters.[1] Recently, much interest was drawn on the use of this material system in the application of tunneling diodes which produce negative differential resistances (NDR).[2-10] New devices incorporating interband tunneling and resonant tunneling were recently demonstrated to have a peak-to-valley current ratio as high as 20 [Ref. 5] at room temperature. In these devices, the operation mechanism is based on the unique feature that the conduction band minimum of InAs is lower than the valence band maximum of GaSb by 0.15 eV.[11] In Ref. 10, we reported the InAs/AlSb/GaSb single-barrier interband tunneling diode. The interband tunneling in this structure was first reported by Takaoka *et al.*[8] Recently, Luo *et al.*[9] demonstrated the NDR characteristics for the first time. The most interesting feature in this structure is that the interband tunneling current is provided by the band overlap between the InAs and the GaSb which offers flexible designs of the barrier widths and the doping concentrations. While in a homojunction tunnel diode, degenerate doping is required to make the tunneling barrier thin enough to obtain significant interband tunneling. In this letter, we study the tunneling characteristics in InAs/AlSb/GaSb single-barrier tunneling diodes as a function of the AlSb barrier thicknesses. The peak current density shows an exponential dependence on the barrier width, which suggests that a simple Wentzel-Kramers-Brillouin (WKB) approximation[12] combined with the $k \cdot p$ two-band model[13] can be used to analyze the energy level in the AlSb barrier through which the peak tunneling currents occur. The significance of the agreement between our calculated energy level and the experimental energy level is the applicability of Kane's $k \cdot p$ two-band model for calculating the wave vector of the tunneling carriers in the InAs/AlSb/GaSb interband tunneling structures.

II. DEVICE FABRICATION

The structure of the InAs/AlSb/GaSb tunneling diode shown in Fig. 1 was grown on a GaAs (100) n^+ substrate in Riber-2300 Molecular Beam Epitaxy (MBE)[14] system. The system is equipped with a solid As cell producing As tetramers, and a cracked Sb cell producing Sb dimers. Growth commenced with a 0.5-μm-thick GaAs buffer layer at 600 °C. The growth was then interrupted, and under As pressure the substrate temperature was lowered to 400 °C. A buffer layer of a 1-μm thick InAs (heavily Si doped) was grown at a growth rate of 0.5 μm/h with a comparable As to In flux ratio. As soon as the InAs growth was initiated, the reflection high-energy electron (RHEED) patterns became spotty, instantly indicating a three-dimensional growth due to a large lattice mismatch (7.2%) between InAs and GaAs. After growing a 20-nm-thick InAs layer, the RHEED changed to streaked (1×1) patterns indicating a smooth two-dimensional growth. This RHEED pattern, corresponding to that of intermediate between (2×4) As stabilized and (4×2) In-stabilized reconstruction, provides good electrical properties.[15] The quality of the InAs film grown on the GaAs substrate was also examined by a double-crystal x-ray diffraction measurement with copper $K_{\alpha 1}$ and $K_{\alpha 2}$ doublet radiation. Figure 2 shows the result from the (400) reflection for the grown film of a 3-μm-thick InAs on a GaAs substrate. Two peaks diffracted from the two source signals can be well resolved for both the substrate and the epitaxial layer, which is indicative of high quality materials. The full width at half maximum (FWHM) diffracted from the $K_{\alpha 1}$ line is 81 arcsec for the substrate and 126 arcsec for the epitaxial layer, which is quite remarkable for the material system with such a large lattice mismatch.

 0021-8979/90/193451-05$03.00 © 1990 American Institute of Physics

[This article is copyrighted as indicated in the article. Reuse of AIP content is subject to the terms at: http://scitation.aip.org/termsconditions. Downloaded to] IP: 128.32.46.241 On: Mon, 21 Jul 2014 20:13:05

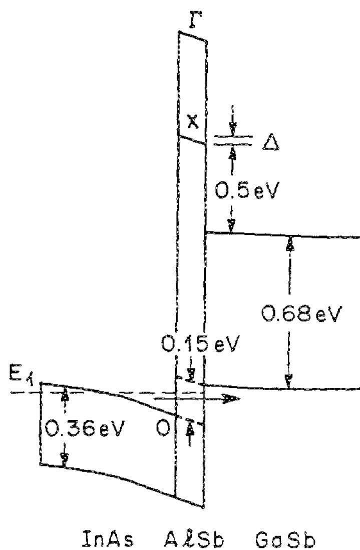

FIG. 1. The band diagrams of a InAs/AlSb/GaSb single barrier tunneling diode at a bias of 0.02 V.

After the growth of a 1-μm-thick n^+ InAs buffer layer, the substrate temperature was raised to 450–500 °C and the whole diode structure was subsequently grown. The structure consisted of a 5-nm-thick undoped InAs, an undoped AlSb with varying thickness, a 5-nm-thick undoped GaSb, and an 80-nm-thick p^+ GaSb contact layer were subsequently grown. Five different widths of the AlSb barrier layer, 5, 3, 1.5, 0.8, and 0 nm were grown to investigate the effect of the barrier on the tunneling current. The undoped InAs layers show n-type background concentrations on the order of 10^{16} cm^{-3} with room-temperature mobilities higher than 1.4×10^4 cm^2/V s. The n^+ InAs layer was doped by Si with a doping concentration about 1×10^{18} cm^{-3}. AlSb and GaSb were grown at a growth rate of 0.5 μm/h with beam equivalent pressure (BEP) ratio of Sb to Al or Ga about 3:1. The undoped GaSb layers were found to be p-type with a typical carrier concentration of about 10^{16} cm^{-3} and room temperature mobility of $(6–10)\times10^2$ cm^2/V s. The p^+ GaSb layer was doped by Be with a doping concentration about 5×10^{18} cm^{-3}. Undoped AlSb layer had a relatively high resistivity on the order of 10^3 Ω cm. All the epitaxial layer thicknesses were precisely confirmed by the cross-sectional transmission electron micrographs (TEM). All the grown samples show mirrorlike surface and smooth interfaces even with a lattice mismatch of 7.2%. The abruptness of the heterojunction was examined by TEM across a large area and was found to be in the atomic range. The diodes with a 60 μm diameter were fabricated by Au/Be/Ti/Au contact metallization, followed by a wet chemical mesa-isolation etching using the metal as an etching mask.
2

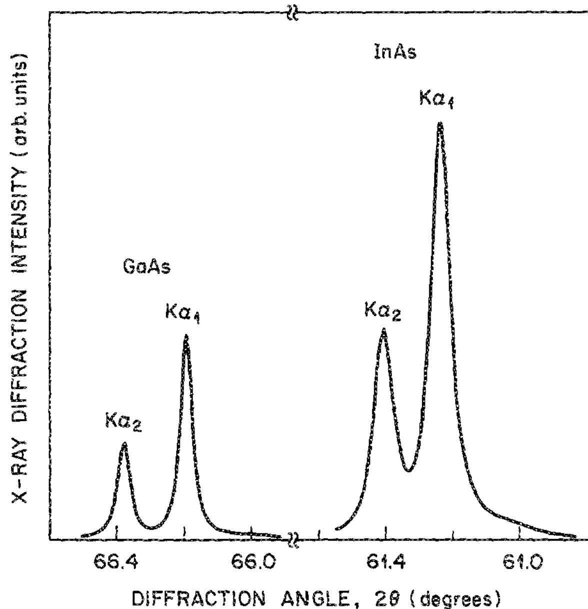

FIG. 2. X-ray diffraction for the (400) reflection of the InAs layer grown on the (100) GaAs substrate.

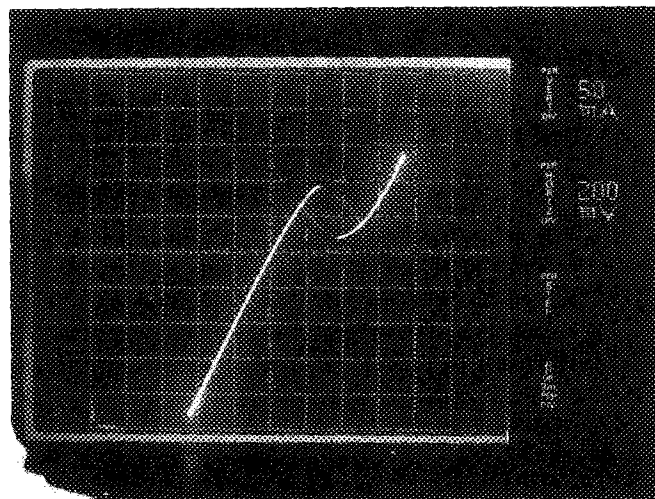

FIG. 3. The current-voltage characteristics of a tunneling diode with a 1.5 nm AlSb barrier.

III. DEVICE CHARACTERIZATION

The band diagram of the single-barrier InAs/AlSb/GaSb tunneling diode with a small forward bias is shown in Fig. 1. At this point, because there are unoccupied states in the valence band of GaSb, the electrons in InAs can tunnel through the AlSb barrier layer into GaSb. However, when the external bias is further increased, the valence band of GaSb is pushed down below the conduction band of InAs. The electrons of the InAs experience a very thick barrier to tunnel through, and the tunneling process is impeded. Figure 3 shows a typical room temperature I-V characteristic of the device with a 1.5-nm-thick AlSb barrier. A distinct negative differential resistance with a peak-to-valley ratio as high as 4.5 can be seen at the forward bias (GaSb positive with respect to InAs). This effect as expected, was not seen in the reverse bias conditions, in contrast to symmetrical barrier devices. A peak current densities of 3.5 kA/cm^2 was observed for this device. The I-V characteristics of the devices with the AlSb barriers 5, 3, and 0.8 nm were also measured at

[This article is copyrighted as indicated in the article. Reuse of AIP content is subject to the terms at: http://scitation.aip.org/termsconditions. Downloaded to] IP: 128.32.46.241 On: Mon, 21 Jul 2014 20:13:05

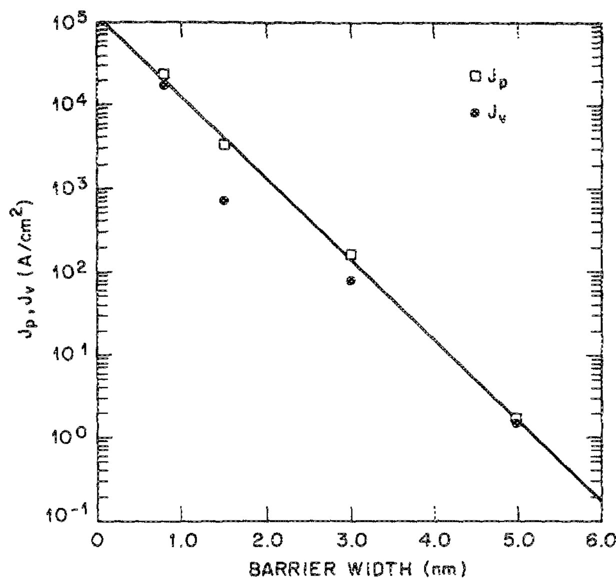

FIG. 4. Dependence of the peak current density and the valley current density at room temperature on the barrier width. The solid line represents a best fit to the experimental peak currents.

room temperature. To make a quantitative comparison, both the peak current densities and the valley current density are plotted as a function of the AlSb barrier widths in Fig. 4. The device with a 0.8-nm-thick AlSb barrier had the highest peak current density of 24 kA/cm^2 while the peak-to-valley ratio was down to 1.4. The device with a 3-nm-thick AlSb barrier had a peak current density of 0.16 kA/cm^2 (PVR = 2). The device with a 5-nm-thick AlSb barrier only showed a shoulder with a current density of 1.68 A/cm^2 (PVR = 2 at 77 K). This relatively low peak current density was due to the reduction of the interband tunneling probability by the thick AlSb barrier layer. In the extreme case of no AlSb barrier ($d = 0$), an ohmic characteristic was observed, consistent with the previous work by Sakaki *et al.*[16] The uniformity of the *I-V* characteristics of these diodes was excellent. All the peak or valley currents found on each sample fell within a 5% variation range.

The values of the peak current density shown in Fig. 4 display an excellent exponential dependence on the AlSb barrier widths. To investigate the effect of the barrier width on the tunneling current, we first discuss the tunneling current which is governed by the following integral:[17]

$$J = A \int [F_c(E) - F_v(E)] n_v(E) T n_c(E) dE, \qquad (1)$$

where A is a constant, T is the tunneling probability, F_c, F_v represent terms of distribution functions as defined in Ref. 17, and n_c, n_v represent the density of states in the conduction band of the InAs and the valence band of the GaSb, respectively. In analyzing the effect of the AlSb barrier on the peak current, we make the following arguments. First, the dependence of the peak current on the barrier width is primarily determined by the tunneling probability T in Eq. (1). Second, the exponential dependence of the peak current on the barrier width in Fig. 4 suggests the usage of the WKB approximation for the tunneling probability. Third, according to our calculation as will be discussed later, at the peak-current bias condition, the potential drop across a 0.8-nm-thick barrier is only 0.012 eV. This small potential drop across the AlSb enables us to use a constant effective wave vector in the WKB approximation. Based on these three arguments, the peak current can be expressed as

$$J \propto \exp(-2\alpha d), \qquad (2)$$

where d is the barrier width and α is the effective value of the wave vector of the carrier in the AlSb barrier. The value of α determined from the slope of the peak current versus the barrier width in Fig. 4 is $(1.106 \pm 0.046) \times 10^9$/m. To obtain the energy level in the AlSb barrier through which the peak tunneling currents occur, we use the dispersion relation using Kane's $k \cdot p$ two-band model[18] given by the following equation:

$$E(1 + E/E_g) = -\hbar^2(1/m_e - 1/m^*)k^2/2, \qquad (3)$$

where E_g is the direct bandgap of the AlSb (2.22 eV), E is the electron energy measured from the conduction band minimum, m_e and m^* are the free and effective mass of electron, respectively. In this calculation, the AlSb light hole mass ($m^* = 0.11 m_e$) was used.[19] The wave vector k will be imaginary for the energies in the forbidden band. By using the effective wave vector $i\alpha$ as k, the value of E_t this obtained was -1.74 ± 0.10 eV (or 0.48 ± 0.10 eV above the valence band maximum of the AlSb). The precision of ± 100 meV is associated with the ± 60 meV uncertainty in measuring the slope of the peak current versus the barrier width, or ± 40 meV assuming 5% uncertainty of the effective mass. This value agrees with the valence-band offset (0.40 ± 0.15 eV) between AlSb and GaSb obtained by x-ray photoemission measurement. While this method may not be the best way to determine the valence-band offset between AlSb and GaSb, our result has the following significance: (a) the agreement

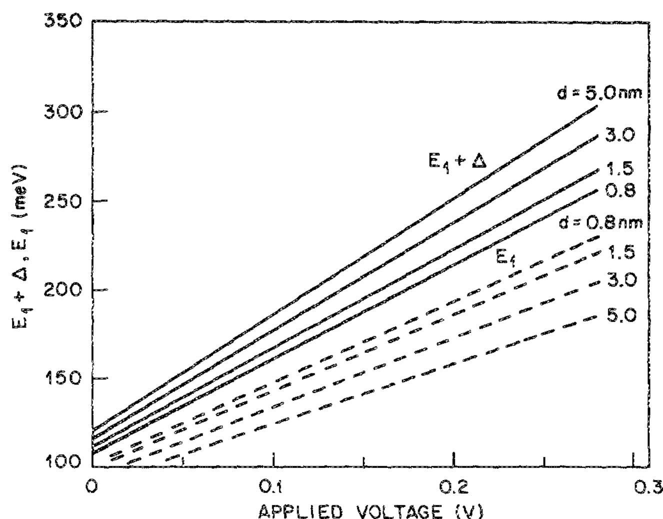

FIG. 5. The subband energy E_1 of the electron in the InAs accumulation region and the sum of E_1 and Δ, the potential drop across the AlSb barrier layer as functions of the external applied voltage for different AlSb barrier width. When $E_1 + \Delta$ exceeds 0.15 eV, the interband tunneling process is cutoff.

[This article is copyrighted as indicated in the article. Reuse of AIP content is subject to the terms at: http://scitation.aip.org/termsconditions. Downloaded to] IP: 128.32.46.241 On: Mon, 21 Jul 2014 20:13:05

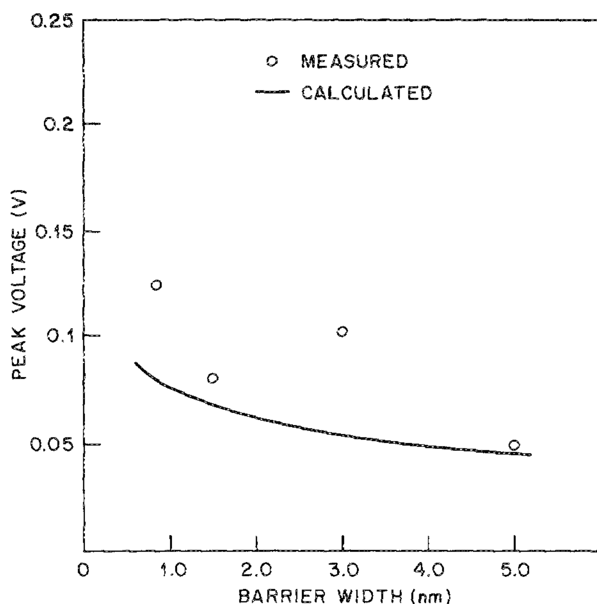

FIG. 6. Dependence of the peak voltage on the barrier width.

between the WKB approximation and the experimental dependence of the peak current on the barrier width; (b) the application of Kane's $k \cdot p$ two-band model in calculating the wave vector of the tunneling carriers. The applicability of the two-band model in calculating the wave vectors of tunneling carriers has been shown in the analysis and demonstration of the InAs/AlGaSb/InAs single-barrier negative differential resistance (NDR) devices.[4,6]

The peak voltage (voltage value at which peak current is observed) was also measured for each device and compared with the predicted values. As a function of applied voltage, the band bending and the associated quantum states are obtained by solving the Schrodinger and Poisson equations self-consistently. The detailed numerical algorithm can be found in Ref. 20. All the physical parameters are taken from Ref. 21. The band overlap of the InAs/GaSb system is assumed to be 0.15 eV. Because the potential barrier formed by AlSb is so large that the calculation results are insensitive to the relative band alignment between AlSb and InAs. In this case, the valence band edge of the AlSb layer is assumed to be aligned with that of the InAs layer as suggested from our results, since their relative locations are not accurately known at present. The calculated quantum states of the first subband E_1 in the InAs triangular potential well for different AlSb barrier widths are shown in Fig. 5 as a function of applied voltage. The results show that at a constant applied voltage, E_1 is smaller for thicker AlSb barrier. Figure 5 also shows the sum of E_1 and Δ, the potential drop across the AlSb barrier. The sum of E_1 and Δ indicates the difference of the first subband of the electron to the valence band of GaSb. When the first subband of the electron in the InAs accumulation region begins to exceed the valence band of the GaSb layer, a cutoff of the interband tunneling process occurs. The predicted cutoff voltages as a function of the AlSb barrier widths are shown in Fig. 6.

The measured peak voltage without any correction from parasitic voltage drops is much larger than the predicted cutoff voltage. At such high peak current densities the parasitic voltage drops due to series resistance (including probe resistance, contact resistance, series resistance of measurement system, substrate resistance) and is the primary reason for this discrepancy. To estimate the parasitic resistance, we measured the resistance of the control diode with no AlSb barrier and found to be 2.2 Ω. We should point out that due to the mismatch of the InAs conduction band and GaSb valence band, wave functions at the InAs/GaSb interface produce a transmission coefficient across the interface that differs significantly from unity, so that the resistance of a device with no AlSb barrier is not exactly equal to just the parasitic resistance. However, the discrepancy of the resistance drop resulting from this effect may be considered to be small compared with some other resistance drops, such as a high resistive interface between the GaAs substrate and the InAs buffer layer. Intrinsic peak voltages for each sample, after subtracting the parasitic resistance drop, are plotted in Fig. 6. Considering the difficulties in obtaining the intrinsic peak voltage, reasonable agreement between the intrinsic peak voltages and the calculated cutoff voltages were obtained, especially for the devices with the 5-nm-thick and 1.5-nm-thick AlSb barriers.

IV. CONCLUSION

In summary, we have investigated the effect of the AlSb barrier layer on the current-voltage characteristics of the InAs/AlSb/GaSb single-barrier interband tunneling structures. We found that the peak current density showed an exponential dependence on the barrier width. The WKB approximation and the $k \cdot p$ two-band model were used to analyze the energy level in the AlSb barrier through which the peak currents occur. The energy level thus obtained agrees with the valence-band offset between the AlSb and the GaSb. In addition, the peak voltages were calculated for different AlSb barrier widths and found to be in agreement with the measured results.

[1] L. Esaki, L. L. Chang, and E. E. Mendez, Jpn. J. Appl. Phys. **20**, L529 (1981).
[2] L. F. Luo, R. Beresford, and W. I. Wang, Appl. Phys. Lett. **53**, 2320 (1988).
[3] R. Beresford, L. F. Luo, and W. I. Wang, Appl. Phys. Lett. **55**, 694 (1989).
[4] J. R. Soderstrom, D. H. Chow, and T. C. McGill, Appl. Phys. Lett. **55**, 1348 (1989).
[5] J. R. Soderstrom, D. H. Chow, and T. C. McGill, Appl. Phys. Lett. **55**, 1094 (1989).
[6] R. Beresford, L. F. Luo, and W. I. Wang, Appl. Phys. Lett. **54**, 1899 (1989).
[7] C. Tejedor, J. M. Calleja, F. Meseguer, E. E. Mendez, C. A. Chang, and L. Esaki, Phys. Rev. B **32**, 5303 (1985).
[8] H. Takaoka, Chin-An Chang, E. E. Mendez, L. L. Chang, and L. Esaki, Physica **117B**, 741 (1983).
[9] L. F. Luo, R. Beresford, and W. I. Wang, Appl. Phys. Lett. **55**, 2023 (1989).
[10] J. F. Chen, M. C. Wu, L. Yang, and A. Y. Cho (unpublished).
[11] L. L. Chang and L. Esaki, Surf. Sci. **98**, 70 (1980).
[12] L. D. Landau and E. M. Lifshitz, *Quantum Mechanics* (Addison-Wesley, MA, 1958), p. 174.
[13] R. A. Smith, *Semiconductor*, 2nd ed. (Cambridge University Press, London, 1979).
[14] A. Y. Cho, Thin Solid Films **100**, 291 (1983).

[This article is copyrighted as indicated in the article. Reuse of AIP content is subject to the terms at: http://scitation.aip.org/termsconditions. Downloaded to] IP: 128.32.46.241 On: Mon, 21 Jul 2014 20:13:05

[15] H. Munekata, T. P. Smith, and L. L. Chang, J. Cryst. Growth **95**, 235 (1989).
[16] H. Sakaki, L. L. Chang, R. Ludeke, C. A. Chang, G. Sai-Halasz, and L. Esaki, Appl. Phys. Lett. **31**, 211 (1977).
[17] L. Esaki, Phys. Rev. **109**, 603 (1958).
[18] E. O. Kane, J. Appl. Phys. **32**, 83 (1961).
[19] M. Cardona, F. H. Pollak, and K. L. Shaklee, Phys. Rev. Lett. **16**, 644 (1966).
[20] L. Yang, M. C. Wu, J. F. Chen, Y. K. Chen, G. L. Snider, and A. Y. Cho (unpublished).
[21] S. M. Sze, *Physics of Semiconductor Devices*, 2nd ed. (Wiley, New York, 1981), p. 849.

[This article is copyrighted as indicated in the article. Reuse of AIP content is subject to the terms at: http://scitation.aip.org/termsconditions. Downloaded to] IP: